University of Nevada, Reno

Thermal Infrared Radiative Forcing By Atmospheric Aerosol

A dissertation submitted in partial fulfillment of
the requirements for the degree of Doctor of
Philosophy in Physics

By

Narayan Adhikari

William P. Arnott, Ph. D. /Dissertation Advisor

August, 2014

2 THEORETICAL ANALYSES OF AEROSOL MICROPHYSICAL AND OPTICAL PROPERTIES

2.1 Size distribution function

The size of particles in the atmosphere usually spans a wide range, which results in a large standard deviation in the normal (Gaussian) distribution for fit of the observed particle sizes. Aerosol size distributions are represented by a normal distribution of the logarithm of the particle radii, called lognormal distribution, in which the natural logarithm of radii is normally distributed (Levoni et al. 1997). The lognormal columnar volume size distribution function $\frac{dV(r)}{d\ln r}$ is given by (Schuster et al. 2006)

$$\frac{dV(r)}{d\ln r} = \frac{C}{\sqrt{2\pi}} \frac{1}{\ln S} \exp\left[-\frac{(\ln r - \ln r_m)^2}{2(\ln S)^2}\right], \tag{2.1}$$

where C represents the column volume of all particles per cross-section of atmospheric column which is obtained by integrating $\frac{dV(r)}{d\ln r}$ over all sizes i.e.

$$C = \int_{r_{min}}^{r_{max}} \frac{dV(r)}{d\ln r} d\ln r. \tag{2.2}$$

This parameter C controls the overall scaling of the distribution. The quantity $\frac{dV(r)}{d\ln r}$ is normalized if C = 1.0. r_m is the volume median, or modal radius; half the particles are smaller and half larger than r_m. The modal radius is the radius of maximum frequency of the distribution. The median and modal radii are identical for lognormal distributions. S is called the geometric standard deviation, which is related to the standard deviation σ of the natural logarithm of the radius lnr (i.e. the radius in log space) by $S = e^{\sigma}$. The dimensionless quantity S gives the spread (or width) of the distribution. The parameters r_m and S are constants for a given size distribution. The values of S (must be ≥ 1) lie in the range 1.5-2.5 for realistic atmospheric aerosols (Zender 2010). For monodisperse particles, S ≈ 1. The factor $\sqrt{2\pi}$ on the denominator comes from the normalization property of the Gaussian function i.e., $\int_{-\infty}^{+\infty} \exp\left(-\frac{x^2}{2}\right) dx = \sqrt{2\pi}$. The common units for the volume distribution dV/dlnr are $\mu m^3\ \mu m^{-2}$. The reason behind the use of volume concentration is that the optical effects of atmospheric aerosols are more related to their volume rather than their number (Whitby 1978).

The columnar particle number size distribution n(r) in the units of number of particles per unit area per size interval in the whole atmosphere column is given by

$$n(r) = \int_0^z N(r, z) dz, \tag{2.3}$$

where $N(r, z)$ is the local number concentration (number per unit volume) per size interval. Assuming spherical particles, we have

$$\frac{\text{total particle volume}}{\text{area of air}} = \int_{r_{min}}^{r_{max}} \frac{dV(r)}{dlnr} dlnr = \int_{r_{min}}^{r_{max}} \frac{4}{3}\pi r^3 n(r) dr = \int_{r_{min}}^{r_{max}} \frac{1}{r} \frac{dV(r)}{dlnr} dr. \tag{2.4}$$

Hence, $n(r)$ is related to the volume size distribution observed by an AERONET Cimel sun-photometer as (Sayer et al. 2012)

$$n(r) = \frac{3}{4\pi r^4} \frac{dV(r)}{dlnr}. \tag{2.5}$$

Eq. 2.5 is used to integrate the individual particle single scattering properties derived from the Mie theory for spherical homogeneous particles (Bohren and Hoffman 1983), or other for non-spherical particles.

Fig. 2.1 depicts examples of measured aerosol bimodal lognormal volume size distributions at the University of Nevada, Reno (UNR), which consist of fine and coarse mode aerosols. The bimodal size distribution can be given by a linear combination of two lognormal functions given by Eq. 2.1 for fine and coarse modes. Fig. 2.1 (left) is a size distribution for a smoke event in Reno on 26 August 2013 at 17:00 Local Standard Time (LST) measured with AERONET (aerosol robotic network) Cimel sun-photometer. The strong predominance of the fine mode implies the presence of small smoke particles. Fig. 2.1 (right) is the aerosol size distribution derived from the MFRSR (multi-filter rotating shadow-band radiometer) data on 24 April 2013 at 14:29 LST during a dust-storm event in Reno. The strong predominating feature of the coarse mode particles over fine (or accumulation) mode is a typical characteristic of a dust outbreak episode (Sicard et al. 2014). The volumetric parameters such as volume median radius, standard deviation and volume concentration for each mode of both dates are reported in Table 2.1. The values of the standard deviation are taken to be 0.42 and 0.61 for the fine and coarse modes, respectively (Dubovik et al. 2002). For the smoke event, the ratio of fine to coarse volume concentration was 10.0, and for the dust event, the coarse to fine volume concentration ratio was 5.3.

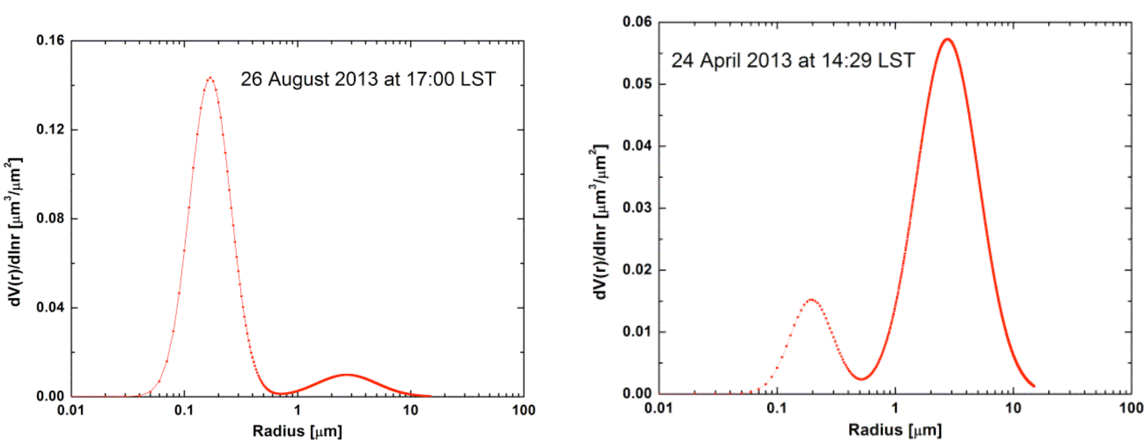

Figure 2.1 Bimodal lognormal aerosol size distributions observed in Reno: (left) during the Rim fire on 26 August 2013 at 17:00 LST measured with the AERONET Cimel sun-photometer and (right) during a dust storm on 24 April 2013 at 14:29 LST derived from the MFRSR data.

Table 2.1 Size distribution function parameters for the Rim fire and dust cases

Particle mode	Concentration (μm^3 μm^{-2})	Median radius (μm)	Standard deviation
Coarse			
26 August 2013	0.015	2.734	0.61
24 April 2013	0.088	2.772	0.61
Fine			
26 August 2013	0.151	0.169	0.42
24 April 2013	0.016	0.196	0.42

2.2 Spectral bulk scattering properties

For a given size distribution n(r), the bulk (or mean) scattering properties at a specific wavenumber ν are obtained by integrating the single scattering properties for individual particles over particle size distribution as follows (Yang et al. 2005; Baum et al. 2006):

$$\langle Q_{ext}(\nu)\rangle = \frac{\int_{r_{min}}^{r_{max}} Q_{ext}(r,\nu)A(r)n(r)dr}{\int_{r_{min}}^{r_{max}} A(r)n(r)dr}, \tag{2.6}$$

$$\langle Q_{sca}(\nu)\rangle = \frac{\int_{r_{min}}^{r_{max}} Q_{sca}(r,\nu)A(r)n(r)dr}{\int_{r_{min}}^{r_{max}} A(r)n(r)dr}, \tag{2.7}$$

$$\langle Q_{abs}(\nu)\rangle = \langle Q_{ext}(\nu)\rangle - \langle Q_{sca}(\nu)\rangle, \tag{2.8}$$

$$\langle \omega(\nu)\rangle = \frac{\langle Q_{sca}(\nu)\rangle}{\langle Q_{ext}(\nu)\rangle}, \tag{2.9}$$

$$\langle g(\nu)\rangle = \frac{\int_{r_{min}}^{r_{max}} g(r,\nu)Q_{sca}(r,\nu)A(r)n(r)dr}{\int_{r_{min}}^{r_{max}} Q_{sca}(r,\nu)A(r)n(r)dr}, \tag{2.10}$$

$$r_{eff} = \frac{3}{4}\frac{\int_{r_{min}}^{r_{max}} V(r)n(r)dr}{\int_{r_{min}}^{r_{max}} A(r)n(r)dr}, \tag{2.11}$$

where $\langle Q_{ext}(\nu)\rangle$, $\langle Q_{sca}(\nu)\rangle$, $\langle Q_{abs}(\nu)\rangle$, $\langle \omega(\nu)\rangle$, and $\langle g(\nu)\rangle$ are the mean extinction efficiency, scattering efficiency, absorption efficiency, single scatter albedo, and asymmetry parameter, respectively. The term r_{eff} is the effective particle radius, or the area-weighted mean radius of an aerosol distribution which characterizes the radiation extinction properties of the distribution. V(r) is the volume of the individual particles and A(r) is the geometric projected area of a particle perpendicular to the incident plane. Similarly, $Q_{ext}(r,\nu)$, $Q_{sca}(r,\nu)$, and $Q_{abs}(r,\nu)$ are the extinction, scattering and absorption efficiencies, respectively, for the individual particles at a specific wavenumber. These quantities are computed using the Mie theory (which is described shortly in brief). The scattering asymmetry parameter is defined as the average value of the cosine of the scattered angle, weighted by the intensity of the scattered radiation as a function of angle. Its value is 1 for perfect forward scattering, -1 for perfect backscatter, and 0 for isotropic scattering.

The scattering phase function $\langle P(\theta,\nu)\rangle$ specifies the fraction of radiation scattered in a certain direction which is given by

$$\langle P(\theta,\nu)\rangle = \frac{\int_{r_{min}}^{r_{max}} P(\theta,r,\nu) Q_{sca}(r,\nu) A(r) n(r) dr}{\int_{r_{min}}^{r_{max}} Q_{sca}(r,\nu) A(r) n(r) dr}. \tag{2.12}$$

The Henyey-Greenstein (H-G) phase function is the most widely used ‘model’ phase function, and is given by (Petty 2006)

$$P_{H-G}(\theta,\nu) = \frac{1-\langle g\rangle^2}{(1+\langle g\rangle^2-2\langle g\rangle\cos\theta)^{\frac{3}{2}}}, \tag{2.13}$$

where θ is the angle between the original direction of the incident photon $\mathbf{\Omega}'$ and the scattered direction $\mathbf{\Omega}$, such that $\cos\theta = \mathbf{\Omega}'.\mathbf{\Omega}$. This function is isotropic for g = 0. For g > 0, the function can reproduce the observed forward peak in the phase functions of real particles.

The parameters Q_{ext}, Q_{sca}, Q_{abs}, and g for a single homogeneous sphere is obtained from the Mie theory in the form of an infinite series (Hansen and Travis 1974):

$$Q_{ext} = \frac{2}{X^2} \sum_{j=1}^{\infty} (2j+1)\, \mathrm{Re}\left(a_j + b_j\right), \tag{2.14}$$

$$Q_{sca} = \frac{2}{X^2} \sum_{j=1}^{\infty} (2j+1) \left(a_j a_j^* + b_j b_j^*\right), \tag{2.15}$$

$$Q_{abs} = Q_{ext} - Q_{sca}, \tag{2.16}$$

$$g = \frac{4}{X^2 Q_{sca}} \sum_{j=1}^{\infty} \left[\frac{j(j+2)}{(j+1)}\, \mathrm{Re}\left(a_j a_{j+1}^* + b_j b_{j+1}^*\right) + \frac{(2j+1)}{j(j+1)} \mathrm{Re}\left(a_j b_j^*\right)\right]. \tag{2.17}$$

The heart of the Mie scattering problem lies in the computation of coefficients a_j and b_j, which are functions of the size parameter x (where $x = \frac{2\pi r}{\lambda}$, and λ is the incident wavelength) and the complex refractive index, and involve spherical Bessel functions. The series converges whenever the number of terms j in the series is slightly larger than x, i.e., j is an integer closest to $(x + 4x^{\frac{1}{3}} + 2)$ (Petty 2006). Higher order terms correspond to light rays missing the sphere. The infinite series actually represents the multipole expansion of the scattered light. The coefficients a_j specify the amounts of electric multipole radiation whereas b_j specify the magnetic multipole radiation. For small particles with a small refractive index, only the electric dipole radiation is significant, and Rayleigh scattering takes place. Fig. 2.2 illustrates the asymmetry parameter for Rayleigh and Mie scatterings. For large particles all multipoles with $j \leq x$ contribute. For much larger particles, usually $x > 2000$, computation of the Mie theory suffers both a computer-time issue and a numerical precision issue due to round-off errors as a consequence of the large value of j.

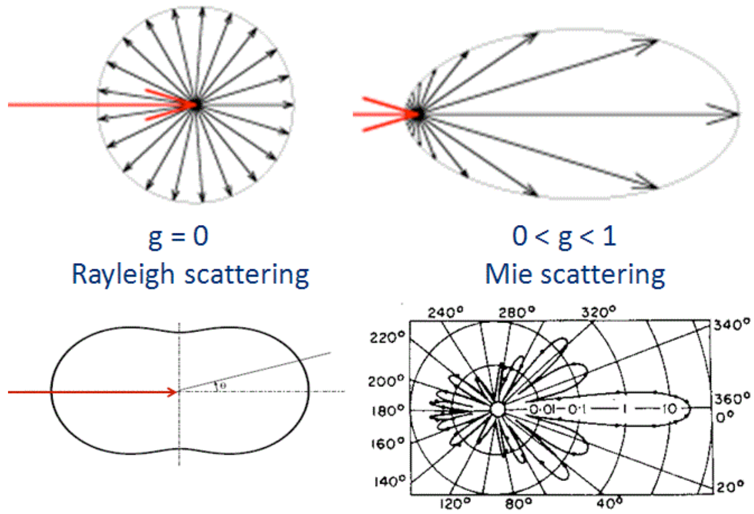

Figure 2.2 Illustration of the phase function for various values of the asymmetry parameter (courtesy: D. Mitchell).

2.3 Physical characteristics of the aerosol problem

This section presents a simple idea about the physical characteristics of the aerosols such as total volume of the aerosols per unit area of the atmospheric column above an instrument. Assume an aerosol-laden atmosphere of volume V observed by an instrument at the surface, whose area is A and height is Z as shown in Fig. 2.3 (left).

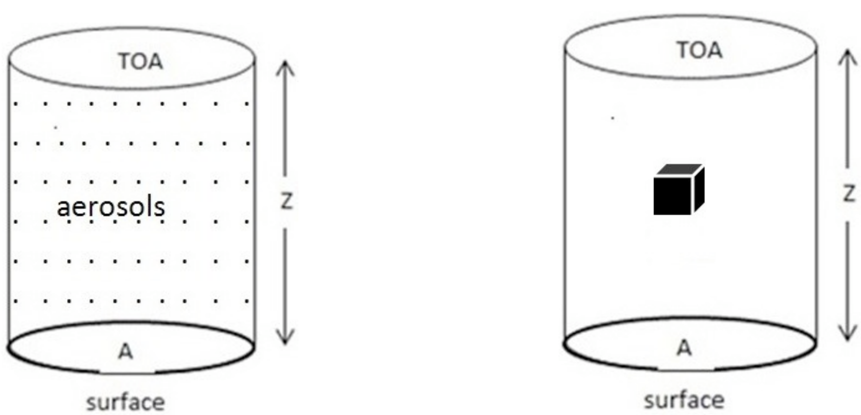

Figure 2.3 Aerosol-laden atmosphere above an instrument at the surface: aerosols distributed over the whole column of the atmosphere (left) and a cube representing the total volume of the aerosols in a unit area (A=1 m^2) of the atmosphere (right).

Referring to the fine mode concentration on 26 August 2013 (Table 2.1), we know that the total volume of all the aerosols present in a column of atmosphere of 1 μm^2 area is 0.151 μm^3, which is equivalent to the volume of 151 mm^3 in an area of 1 m^2. This is, in fact, the volume of all aerosol particles when gathering them together in an area of a unit square meter (Fig. 2.3, right, where A is assumed to be 1 m^2). This volume then represents a cube of side 5.3 mm in this particular case. Is it not a tiny volume of matter dispersed into the whole column of the atmosphere, which we are dealing with?

2.4 Pedagogical model for IR radiative forcing by aerosols

We consider a simplified atmosphere containing water vapor and coarse mode aerosols such as mineral dust (Fig. 2.4) where dust resides only in the boundary layer (0-3 km). Let T be the surface temperature and T_a be the atmospheric temperature.

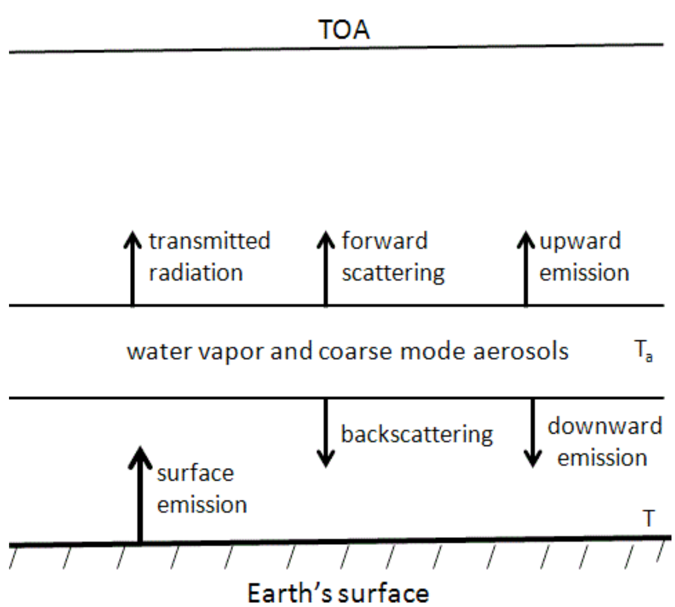

Figure 2.4 A simplified atmosphere containing water vapor and coarse mode aerosols.

The radiance at the TOA is given by

$$R_{TOA}(\nu) = B(T,\nu)\exp[-(\tau_{abs}^{H_2O} + \tau_{ext}^{dust})] + B(T_a,\nu)[1 - \exp\{-(\tau_{abs}^{H_2O} + \tau_{abs}^{dust})\}] +$$
$$B(T)\,\tau_{sca}^{dust}\left(\frac{1+g}{2}\right)\exp(-\tau_{abs}^{H_2O}), \qquad (2.18)$$

where ν is the wavenumber; B is the Planck's function; $\tau_{abs}^{H_2O}$ is the absorption optical depth of water vapor; τ_{ext}^{dust} , τ_{abs}^{dust}, and τ_{sca}^{dust} are the extinction, absorption and scattering optical depths, respectively of coarse mode aerosol such as dust; and $\left(\frac{1+g}{2}\right)$ represents the probability of scattering in the forward direction. Similarly the radiance at the BOA is given by

$$R_{BOA}(\nu) = B(T_a,\nu)\left[1 - \exp\left\{-\left(\tau_{abs}^{H_2O} + \tau_{abs}^{dust}\right)\right\}\right] + B(T)\,\tau_{sca}^{dust}\left(\frac{1-g}{2}\right)\exp\left(-\tau_{abs}^{H_2O}\right), \qquad (2.19)$$

where $\left(\frac{1-g}{2}\right)$ represents the probability for backward scattering. The second term in Eq. 2.19, therefore, signifies the surface IR backscattering by atmospheric dust.

The spectral radiative forcing at the TOA, $\Delta R_{TOA}(\nu)$ is obtained by subtracting $R_{TOA}(\nu)$ with dust from $R_{TOA}(\nu)$ without dust. Therefore,

$$\Delta R_{TOA}(\nu) = B(T)\exp\left(-\tau_{abs}^{H_2O}\right)\left[1 - \exp\left(-\tau_{ext}^{dust}\right)\right] - B(T_a)\exp\left(-\tau_{abs}^{H_2O}\right)\left[1 - \exp\left(-\tau_{abs}^{dust}\right)\right] - B(T)\,\tau_{sca}^{dust}\left(\frac{1+g}{2}\right)\exp\left(-\tau_{abs}^{H_2O}\right). \qquad (2.20)$$

Assuming τ_{ext}^{dust} and τ_{abs}^{dust} are far less than 1, then Eq. 2.20 can be written as

$$\Delta R_{TOA}(\nu) = \exp\left(-\tau_{abs}^{H_2O}\right)\left[B(T)\,\tau_{ext}^{dust} - B(T_a)\,\tau_{abs}^{dust}\right] - B(T)\,\tau_{sca}^{dust}\left(\frac{1+g}{2}\right)\exp\left(-\tau_{abs}^{H_2O}\right). \qquad (2.21)$$

Using $\omega = \frac{\tau_{sca}^{dust}}{\tau_{ext}^{dust}}$ i.e., single scattering albedo, we have

$$\Delta R_{TOA}(\nu) = \exp\left(-\tau_{abs}^{H_2O}\right)\left[B(T)\,\tau_{ext}^{dust}\left\{1 - \frac{\omega(1+g)}{2}\right\} - B(T_a)\,\tau_{abs}^{dust}\right]. \qquad (2.22)$$

In the limit, $\omega \approx 0$, i.e., zero scattering approximation

$$\Delta R_{TOA}(\nu) = \tau_{abs}^{dust}\exp\left(-\tau_{abs}^{H_2O}\right)\left[B(T) - B(T_a)\right]. \qquad (2.23)$$

We see that, for a large value of $\tau_{abs}^{H_2O}$ (i.e. moist atmosphere), the dust radiative forcing at the TOA, $\Delta R_{TOA}(\nu)$ becomes small. Also, the forcing decreases with increasing atmospheric temperature T_a. In the limit, $\omega \approx 1$ i.e., zero absorption approximation

$$\Delta R_{TOA}(\nu) = \exp\left(-\tau_{abs}^{H_2O}\right)B(T)\left(\frac{1-g}{2}\right)\tau_{sca}^{dust}. \qquad (2.24)$$

Apparently the backscattering of the surface-emitted IR by the dust causes the radiative forcing to be important. If $\Delta R_{TOA}(\nu) > 0$, less IR leaves at TOA in the presence of dust and hence the atmosphere gets heated. Using $\tau_{abs}^{dust} = (1-\omega)\tau_{ext}^{dust}$, Eq. 2.22 can be re-written generally as

$$\Delta R_{TOA}(\nu) = B(T)\,\tau_{ext}^{dust}\exp\left(-\tau_{abs}^{H_2O}\right)\left[1 - \frac{\omega(1+g)}{2} - (1-\omega)\frac{B(T_a)}{B(T)}\right]. \qquad (2.25)$$

The spectral radiative forcing at the BOA, $\Delta R_{BOA}(\nu)$ due to dust is obtained by subtracting $R_{BOA}(\nu)$ without dust from $R_{BOA}(\nu)$ with dust i.e.

$$\Delta R_{BOA}(\nu) = B(T_a)\exp\left(-\tau_{abs}^{H_2O}\right)\left[1 - \exp\left\{-(1-\omega)\,\tau_{ext}^{dust}\right\}\right] + B(T)\,\omega\,\tau_{ext}^{dust}\left(\frac{1-g}{2}\right)\exp\left(-\tau_{abs}^{H_2O}\right).$$

Assuming small τ_{ext}^{dust} , we have

$$\Delta R_{BOA}(\nu) = B(T)\,\tau_{ext}^{dust}\exp\left(-\tau_{abs}^{H_2O}\right)\left[\omega\left(\frac{1-g}{2}\right) + (1-\omega)\frac{B(T_a)}{B(T)}\right]. \qquad (2.26)$$

Notice that $\frac{B(T_a)}{B(T)} \sim \frac{T_a^4}{T^4}$, and $\frac{T_a^4}{T^4} \approx \left(1 - \frac{\Delta T}{T}\right)^4 \approx 1 - 4\frac{\Delta T}{T}$. Then

$$\Delta R_{BOA}(\nu) \approx B(T)\,\tau_{ext}^{dust}\exp\left(-\tau_{abs}^{H_2O}\right)\left[\omega\left(\frac{1-g}{2}\right) + (1-\omega)\left(1 - 4\frac{\Delta T}{T}\right)\right]. \qquad (2.27)$$

For the zero aerosol absorption and emission case, $\omega = 1$,

$$\Delta R_{BOA}(\nu) = B(T)\,\tau_{ext}^{dust}\exp\left(-\tau_{abs}^{H_2O}\right)\left(\frac{1-g}{2}\right). \qquad (2.28)$$

Even though the dust aerosols do not absorb IR at all, the backscattering of IR by the aerosols contributes to IR radiative forcing. Also, the aerosol IR radiative forcing enhances in the drier atmosphere. This offers positive feedback on the climate warming. For a warmer planet, $B(T)$ goes up and contributes to the positive feedback. For $\omega \approx 0$,

$$\Delta R_{BOA}(\nu) = B(T_a)\,\tau_{abs}^{dust}\exp\left(-\tau_{abs}^{H_2O}\right). \qquad (2.29)$$

Eq. 2.29 is the zero scattering approximation, which can be used to investigate the perturbation due to any other greenhouse gas. The approximate forcings given in Eqs. 2.25 and 2.26 were also presented by Dufresne et al. 2002, though without the dependence on water vapor optical depth.